

This article was downloaded by:

On: 23 January 2011

Access details: *Access Details: Free Access*

Publisher *Taylor & Francis*

Informa Ltd Registered in England and Wales Registered Number: 1072954 Registered office: Mortimer House, 37-41 Mortimer Street, London W1T 3JH, UK



## Journal of Coordination Chemistry

Publication details, including instructions for authors and subscription information:

<http://www.informaworld.com/smpp/title~content=t713455674>

### The Binding Affinity of Fe(III) to Aspartic Acid and Glutamic Acid Monohydroxamates

Nadia M. Shuaib<sup>a</sup>; Hayat M. Marafie<sup>a</sup>; Hamido Ben Youngo<sup>a</sup>; Fawzia M. Al-Sogair<sup>b</sup>; Mohamed S. El-Ezaby<sup>c</sup>

<sup>a</sup> Chemistry Department, Kuwait University, Safat, Kuwait <sup>b</sup> Faculty of Medicine, King Faisal University, Saudi Arabia <sup>c</sup> Gulf Institute of Science and Technology, Safat, Kuwait

Online publication date: 15 September 2010

**To cite this Article** Shuaib, Nadia M. , Marafie, Hayat M. , Youngo, Hamido Ben , Al-Sogair, Fawzia M. and El-Ezaby, Mohamed S.(2002) 'The Binding Affinity of Fe(III) to Aspartic Acid and Glutamic Acid Monohydroxamates', *Journal of Coordination Chemistry*, 55: 8, 933 – 949

**To link to this Article:** DOI: 10.1080/0095897022000002268

**URL:** <http://dx.doi.org/10.1080/0095897022000002268>

PLEASE SCROLL DOWN FOR ARTICLE

Full terms and conditions of use: <http://www.informaworld.com/terms-and-conditions-of-access.pdf>

This article may be used for research, teaching and private study purposes. Any substantial or systematic reproduction, re-distribution, re-selling, loan or sub-licensing, systematic supply or distribution in any form to anyone is expressly forbidden.

The publisher does not give any warranty express or implied or make any representation that the contents will be complete or accurate or up to date. The accuracy of any instructions, formulae and drug doses should be independently verified with primary sources. The publisher shall not be liable for any loss, actions, claims, proceedings, demand or costs or damages whatsoever or howsoever caused arising directly or indirectly in connection with or arising out of the use of this material.

## THE BINDING AFFINITY OF Fe(III) TO ASPARTIC ACID AND GLUTAMIC ACID MONOHYDROXAMATES

NADIA M. SHUAIB<sup>a</sup>, HAYAT M. MARAFIE<sup>a\*</sup>, HAMIDO BEN YOUNGO<sup>a</sup>,  
FAWZIA M. AL-SOGAIR<sup>b</sup> and MOHAMED S. EL-EZABY<sup>c,\*</sup>

<sup>a</sup>*Chemistry Department, Kuwait University, P.O. Box 5969 Safat, 13060 Kuwait;*

<sup>b</sup>*Faculty of Medicine, King Faisal University, Al-Dammam, P.O. Box 2114, Saudi Arabia;*

<sup>c</sup>*Gulf Institute of Science and Technology, P.O. Box 29623, Safat, 13157 Kuwait*

*(Received 9 February 2001; Revised on 15 May 2001; In final form 10 October 2001)*

The solution spectra of Fe(III) complexes with aspartic acid (ASX) and glutamic acid (GLX) monohydroxamates were analyzed in the UV–Vis region for different complex species using STAR-94 programs in the pH range ~1.0–4.0, at ionic strength (*I*) of 0.15 M NaCl and *T* = 25°C. Several monomeric complex species were obtained including some mixed hydroxo species. The reaction kinetics of the Fe(III)-(ASX or GLX) systems were carried out at *I* = 0.15 M NaCl and *T* = 25°C in the time range of the stopped-flow method. The pseudofirst-order rate constants were pH as well as *T*<sub>L</sub> (analytic concentration of ASX or GLX) dependent, i.e.

$$k_{\text{obs},i} = A_i + B_i T_L \text{ (at a given pH}_i\text{)}$$

where *A<sub>i</sub>* and *B<sub>i</sub>* are pH-dependent parameters.

*Keywords:* Hydroxamates; Fe(III); Formation constants; Rate constants

### INTRODUCTION

The essentiality of Fe(III) to living systems has been known for a long time [1]. A variety of means for acquisition, uptake, and storage of the element have been developed by living cells to ensure a supply of this essential element [2]. Since Fe(III) is usually found in polymeric form in solutions of pH's > 1, solubilization of insoluble iron polymers is the first step in iron assimilation. The two methods most commonly utilized by living cells for solubilization of iron are reduction and chelation. Siderophores [3,4] are among many chelators which facilitate the acquisition of Fe(III) from the cell environment. They vary greatly in structure, but have some common features such as catechol or hydroxamate groups as Fe(III) binding sites. The cellular acquisition or release of

---

\*Corresponding authors. E-mail: ezabyh@chemist.moc

Fe(III) depends to an extent on the thermodynamic and kinetic properties of the complex formation with the siderophores. As a model of hydroxamate siderophores of the multidentate nature, aspartic- $\beta$ -hydroxamate and glutamic- $\gamma$ -hydroxamate have been selected to study their reaction kinetics and equilibria with Fe(III).

## EXPERIMENTAL

Stock solutions of monohydroxamates (99% Sigma) were prepared in acidic media of equal concentration (0.01 M). Stock solutions of known concentration of ferric chloride (E-Merck) (0.10 M) were also prepared in acidic media of equal HCl concentration or more. The concentration of Fe(III) was checked complexometrically by standard EDTA titration using salicylate as indicator in acidic media [5]. Potentiometric titrations of the ligands were done by using a Metrohm automatic titrator model 716 DMS Titrino with 727 titrator stand provided by Metrohm glass and Ag/AgCl reference electrodes. The titrator was calibrated by three standard buffers (4.00, 7.00, 10.00) as well as by titrating standard HCl solution (0.10 M) against standard carbonate free NaOH (0.097 M) at  $I = 0.15$  M NaCl and  $T = (25 \pm 0.01)^\circ\text{C}$ . The calculated pH values were different by only  $\sim 0.016$  pH unit from the measured values. The titration experiments were run under humidified pure nitrogen (99.999%) in the pH range  $\sim 2$ –11,  $I = 0.15$  M NaCl, and at  $T = (25 \pm 0.01)^\circ\text{C}$  using always freshly prepared solutions of the ligands, especially for GLX. The titrant was carbonate free NaOH in 0.15 M NaCl. The equilibration period did not exceed 5 s after the addition of 0.04 mL increments of the titrant. However, readings were taken 40 s after addition of the titrant increments.

The absorption spectra were taken using a Cary 500 spectrophotometer in the wavelength range 250–650 nm at different values of pH and various initial concentrations of Fe(III) ( $T_{\text{Fe}}$ ) and ligands ( $T_{\text{L}}$ ) such that  $T_{\text{L}}$  was at least ten times  $T_{\text{Fe}}$ . The  $T_{\text{Fe}}$  did not exceed  $4 \times 10^{-4}$  M.

Kinetic measurements were done using an Applied Photophysics stopped-flow sequential spectrometer model DX-17mV provided with a 15–109 spectrakinetic monochromator. The concentrations of the ligands were in the range of  $(1\text{--}6) \times 10^{-3}$  M and that of Fe(III) was kept constant at  $1 \times 10^{-4}$  M. There was no indication of precipitation in the pH ranges up to  $\text{pH} \sim 4.0$ . The temperature was kept constant at  $(25 \pm 0.1)^\circ\text{C}$  and the ionic strength ( $I$ ) was adjusted to 0.15 M NaCl. *Pseudo* first-order conditions were maintained in the kinetic study as previously described [6].

The protonation constants of the ligands were calculated by the program SUPERQUAD as previously reported [7]. The obtained values are listed in Table I. The formation constants as well as the stoichiometries of Fe(III)-ASX or Fe(III)-GLX systems were calculated by STAR-94 programs [8].

## RESULTS AND DISCUSSION

Fe(III) reacts with the ligands ASX or GLX in acidic media producing strong red coloration. The absorption spectra in the 250–650 nm wavelength range and in the pH range  $\sim 1.0$ – $\sim 4.0$ , are shown in Fig. 1(a,b). As the pH increased, there is a gradual decrease in absorbance at  $\sim 325$  nm, where free Fe(III) absorbs. At the same time,

TABLE I Summary of the overall formation constants encountered in the Fe(III)-ASX and GLX systems, where  $p$ ,  $q$ , and  $r$  are the stoichiometric coefficients for the species (ASX or GLX) $_p$  Fe $_q$  H $_r$

System	Stoichiometric coefficients			Log $\beta_{pqr}$ ( $\pm\sigma$ )	pH range used	Reported values <sup>c</sup>
	$p$	$q$	$r$			
ASX-H <sup>a</sup>	1	0	1	9.14 $\pm$ 0.01	~2.0–10.5	9.37
	1	0	2	16.51 $\pm$ 0.01		17.52
	1	0	3	19.83 $\pm$ 0.01		19.70
GLX-H <sup>a</sup>	1	0	1	9.73 $\pm$ 0.02		9.50
	1	0	2	18.28 $\pm$ 0.02		18.03
	1	0	3	20.55 $\pm$ 0.02		20.26
Fe-OH <sup>f</sup>	0	1	-1			-3.05
	0	1	-2			-6.31
	0	2	-2			-2.79
	0	0	-1			13.76
Fe(III)-ASX <sup>b</sup>	1	1	0	21.06 $\pm$ 0.16 <sup>c</sup>	~1.0–3.0	—
	2	1	0	37.93 $\pm$ 0.03		24.25 <sup>a</sup>
	1	1	1	22.42 $\pm$ 0.18		18.82
	2	1	2	42.03 $\pm$ 0.04		36.35
	2	1	-1	34.88 $\pm$ 0.05		15.32
	3	1	-2	45.36 $\pm$ 0.05		—
	2	1	1	—		31.63
Fe(III)-GLX <sup>b</sup>	1	1	0	21.91 $\pm$ 0.02 <sup>d</sup>		—
	1	1	1	23.06 $\pm$ 0.03		18.92 <sup>a</sup>
	2	1	1	41.02 $\pm$ 0.06		31.70
	1	1	-2	17.78 $\pm$ 0.08		—
	2	1	-2	31.39 $\pm$ 0.07		—
	3	1	-2	45.07 $\pm$ 0.03		—
	2	1	-1	—		14.70
	2	1	0	—		24.10
	2	1	2	—		36.65

<sup>a</sup>Pot.: potentiometric; <sup>b</sup>Spec.: spectrophotometric; <sup>c</sup>Residual mean of absorbance values = 0.0003; Chi-squared test = 36.6; Hamilton R-factor = 1.26; <sup>d</sup>Residual mean of absorbance values = 0.0004; Chi-squared test = 83.3; Hamilton R-factor = 1.24; <sup>e</sup>Ref. 9; <sup>f</sup>Ref. 12.

a new broad band at  $\lambda \sim 500$  nm appeared associated with appreciable increase in absorbance and slight blue shift of the wavelength maxima as pH was increased. These findings were appropriate to determine the number of the absorbing species and their formation constants using STAR-94 programs.

Table I, lists the protonation constants of the hydroxamates. Small differences in the protonation constants of ASX and GLX were observed. The structure of both hydroxamates differ only by an extra CH<sub>2</sub>-group attached to the stereogenic carbon in the case of glutamate- $\gamma$ -hydroxamate. The calculated formation constants of the Fe(III)-ASX and Fe(III)-GLX complexes and their stoichiometries are also reported in Table I. The pH range used was  $\sim 1.0$ – $3.0$  and the wavelength range was 355–600 nm. The molar absorptivity of free aquated Fe(III) species, mainly Fe<sup>3+</sup>, in the wavelength range used was taken into consideration in the calculation of the formation constants of the complex species. In addition, the protonation constants of the ligands were kept constant while refining the formation constants of the complex species. On the other hand the hydrolysis constants of Fe(III) were also kept constant in the refinement based on the fact that the  $T_L \gg T_{Fe}$ , avoiding the formation of appreciable concentration of Fe(III) hydrolyzed species.

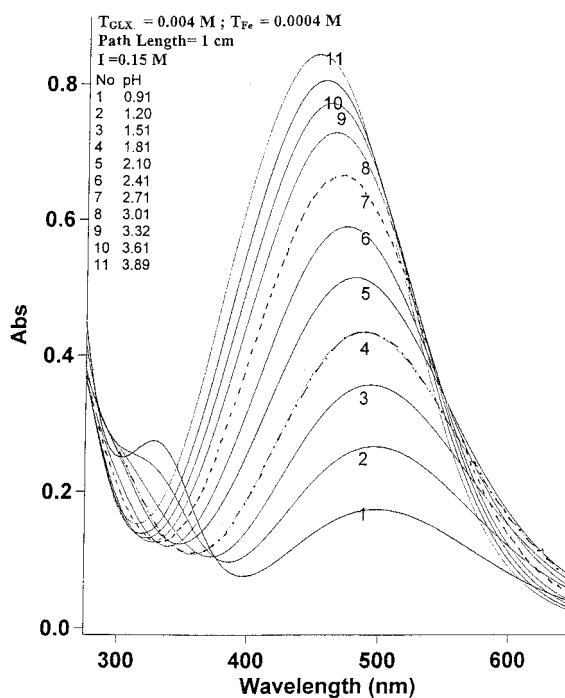
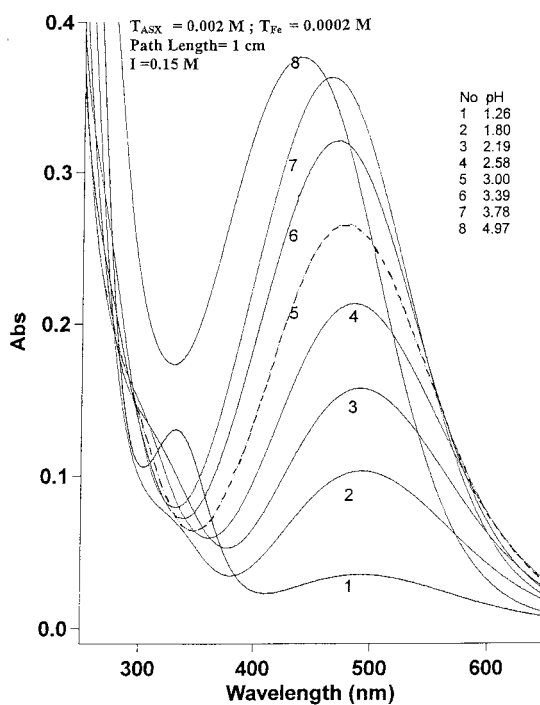


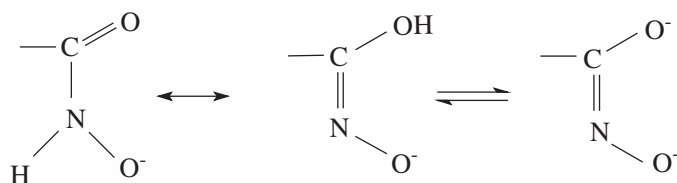
FIGURE 1 (a) Representative spectra of Fe(III)-ASX system; (b) Representative spectra of Fe(III)-GLX system.

## Equilibrium Studies

Several models were used to simulate the equilibria using the STAR-94 program. The model which was selected complies with the lowest values of the statistical parameters provided with the program. The selection was also based on the chemical nature of the metal and the ligands and on the reliability of the complex species. In addition, the calculated spectra were found to be compatible with the experimental spectra.

The discrepancies between the values reported in this work and the literature values [9] may be attributed to the experimental method used. The literature values were from potentiometric methods where Fe(III) hydrolysis is prominent; there was no mention of the effect of Fe(III) hydrolysis on the results in this report. In spectrophotometric methods of analysis excess ligand concentration to that of the metal is not a hindering factor as in the potentiometric methods. In addition, it has been reported [10] that hydroxamates are susceptible to deterioration in acidic solution by time. There is no mention in the literature report about the effect of time on hydroxamates in solution. In the current work freshly prepared solutions were always used.

Figure 2(a,b) shows the species distribution curves of the complex species in both systems as a function of pH. The ASX system is not completely comparable with the GLX system in the composition of the complex species which may indicate different ligating properties of ASX and GLX. Both ligands have the same ligating sites, the oxygens of the carboxylate group, the nitrogen of the amino group, and both nitrogen and oxygen atoms of the hydroxamate group. Being a hard metal ion, Fe(III) is ligated through the oxygen sites of these ligands forming different possibilities in which the ligands may act as bidentate (using the two oxygen sites of the hydroxamate group) or tridentate ligands utilizing, in addition, the oxygen sites of the hydroxamate group and carboxylate group. However, ASX exhibits more steric hinderance than GLX, when behaving as a tridentate ligand.



The ratios {ASX or GLX:Fe(III):H<sup>+</sup>} of (1:1:-2), (2:1:-2), (2:1:-1), and (3:1:-2) complex species which are found to exist at pH values > 1.5 in both systems may be explained as either due to the formation of hydroxo species of the complex or due to the deprotonation of NH proton of the hydroxamate group which is usually undissociable in acidic media (i.e. pK probably > 13.00). The formation of the hydroxo species can be predicted on the basis that Fe(III) can be hydrolyzed in acidic media specially at pH values > 1.0. However, this argument is against the aforementioned experimental condition where excess ligand was used. The other suggestion is feasible, due to the high polarizing effect of Fe(III), the ionization of NH proton of the hydroxamate group in acidic medium is possible. This, of course, will lead to a greater thermodynamic stability. Both systems show the formation of (3:1:-2) complex species which is peculiar to the octahedral structure of Fe(III) if the tridentate nature of the ligands is assumed. However, to keep the octahedral properties of Fe(III)

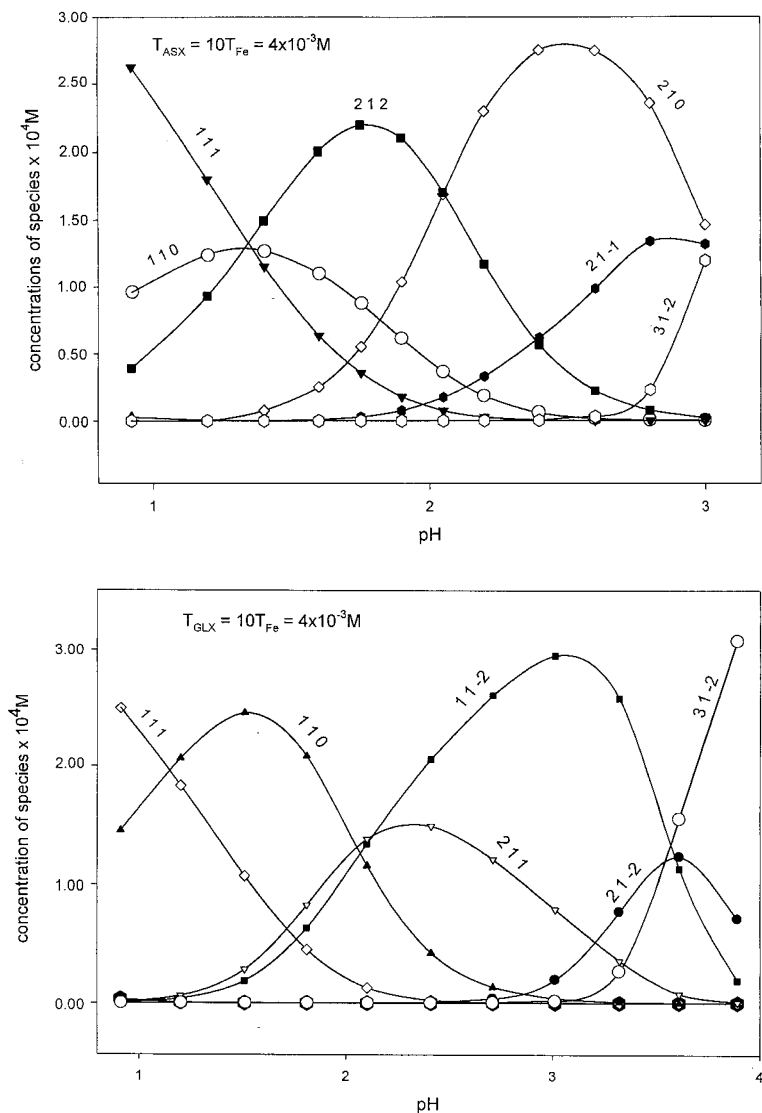


FIGURE 2 (a) STAR-94 distribution diagram of the species in the Fe(III)-ASX system; (b) STAR-94 distribution diagram of the species in the Fe(III)-GLX system.

complexes, one may visualize that the ligands are mainly bidentate in nature with further loss of a proton from the NH moiety of the hydroxamate group.

## KINETIC STUDY

### Kinetic of Fe(III)-ASX System

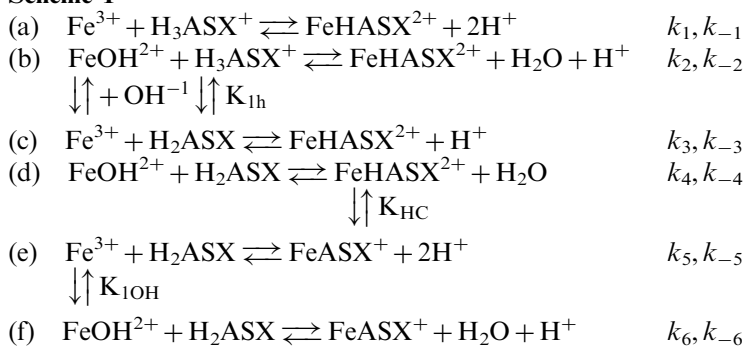
The interaction of Fe(III) with ASX under *pseudo* first-order reaction conditions ( $T_{\text{ASX}} \gg T_{\text{Fe}}$ ) showed one rate step in the millisecond range at 450 nm. The rate step

was attributed to the formation of Fe(III) complexes with ASX. In this study the concentration of Fe(III) was kept at  $1.0 \times 10^{-4}$  M. Figure 3(a,b) shows the dependence of the observed rate constants  $k_{\text{obs}}$ , on both pH and  $T_{\text{ASX}}$ . They were first decreased as pH increased from  $\sim 1.0$  up to  $\sim 1.4$  (depending on the value of  $T_{\text{ASX}}$ ) and then increased as the pH increased from  $\sim 1.4$ – $\sim 2.3$ . At a given pH the observed rate constant is linear function of  $T_{\text{ASX}}$ , Fig. 4(a,b). The two sets of curves have significant slopes and intercepts in the pH range  $\sim 1.0$ – $\sim 2.3$ , Table II. Both sets of curves could be represented empirically by the following equation:

$$k_{\text{obs},i} = A_i + B_i T_{\text{ASX}} \quad (\text{at pH}_i) \quad (1)$$

Where  $A_i$  and  $B_i$  are the intercepts and slopes of the linear plots shown in Fig. 4(a,b). Since the main species of Fe(III) are the aquated species of  $\text{Fe}^{3+}$ ,  $\text{FeOH}^{2+}$ , and  $\text{Fe}(\text{OH})_2^+$ , and those of ASX are  $\text{H}_3\text{ASX}^+$  and  $\text{H}_2\text{ASX}$  in the pH range used, one can derive the mechanism of the reactions of Fe(III) with ASX described in Scheme 1 where the contribution of  $\text{Fe}(\text{OH})_2^+$  reaction to the mechanism is ignored since the reactions started at pH values  $< 1.0$ .

#### Scheme 1



Where  $k_i$  and  $k_{-i}$  are the forward and backward rate constants.

At a given pH, the rate equation can be expressed as follows (refer to the appendix for more details) where some of the charges are omitted for simplicity:

$$d((\text{FeASX})/dt) = T_{\text{ASX}}(T_{\text{Fe}}Q_4/Q_3Q_2) - (\text{FeASX})((T_{\text{ASX}}Q_2Q_4/Q_3)Q_5) + Q_2 \quad (2)$$

where:

$$\begin{aligned}
 T_{\text{ASX}} &\approx \sum_{i=0-3} [\text{ASXH}_i], \\
 T_{\text{Fe}} &= \sum_{i=0,1, j=0,1, k=0,1} [\text{Fe}(\text{OH})_i(\text{ASX})_j(\text{H}^+)_k], \\
 Q_1 &= (\text{H}^+)^3 + K_{1h}(\text{H}^+)^2 + K_{1h}K_{2h}(\text{H}^+) \\
 &\quad + K_{1h}K_{2h}K_{3h} \approx (\text{H}^+)^3 + K_{1h}(\text{H}^+)^2 \quad \{\text{in the pH range used}\}
 \end{aligned}$$

((where  $K_{1h}$ ,  $K_{2h}$  and  $K_{3h}$  are the deprotonation constants of  $(\text{H}_3\text{ASX})$  species ( $\text{p}K_1 = 3.32$ ,  $\text{p}K_2 = 7.37$  and  $\text{p}K_3 = 9.14$ )),  $Q_2 = (1 + K_{\text{HC}}(\text{H}^+))$  (where  $K_{\text{HC}}$  is the protonation



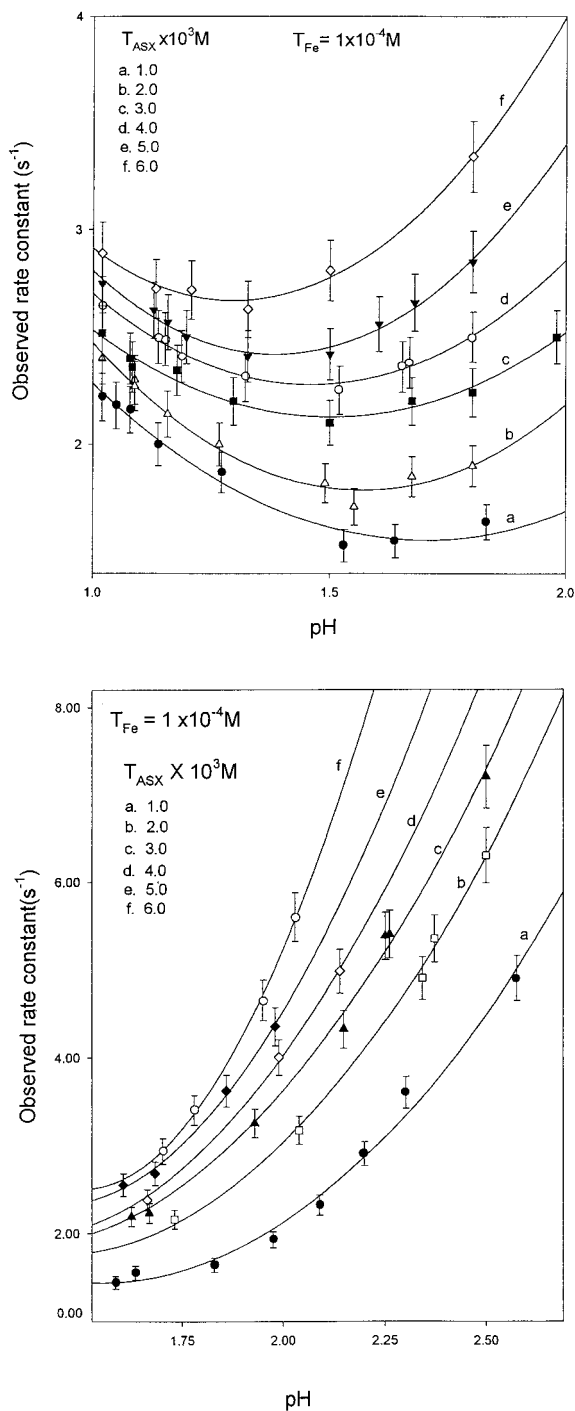


FIGURE 3 (a) The variation of  $k_{\text{obs}}$  as function of pH at a fixed wavelength (= 450 nm), constant  $I$  (0.15 M NaCl) and constant  $T$  (25°C) at pH values < 1.5 and different  $T_{\text{ASX}}$  for Fe(III)-ASX system; (b) The variation of  $k_{\text{obs}}$  as function of pH at a fixed wavelength (= 450 nm), constant  $I$  (0.15 M NaCl) and constant  $T$  (25°C) at pH values > 1.5 and different  $T_{\text{ASX}}$  for Fe(III)-ASX system.

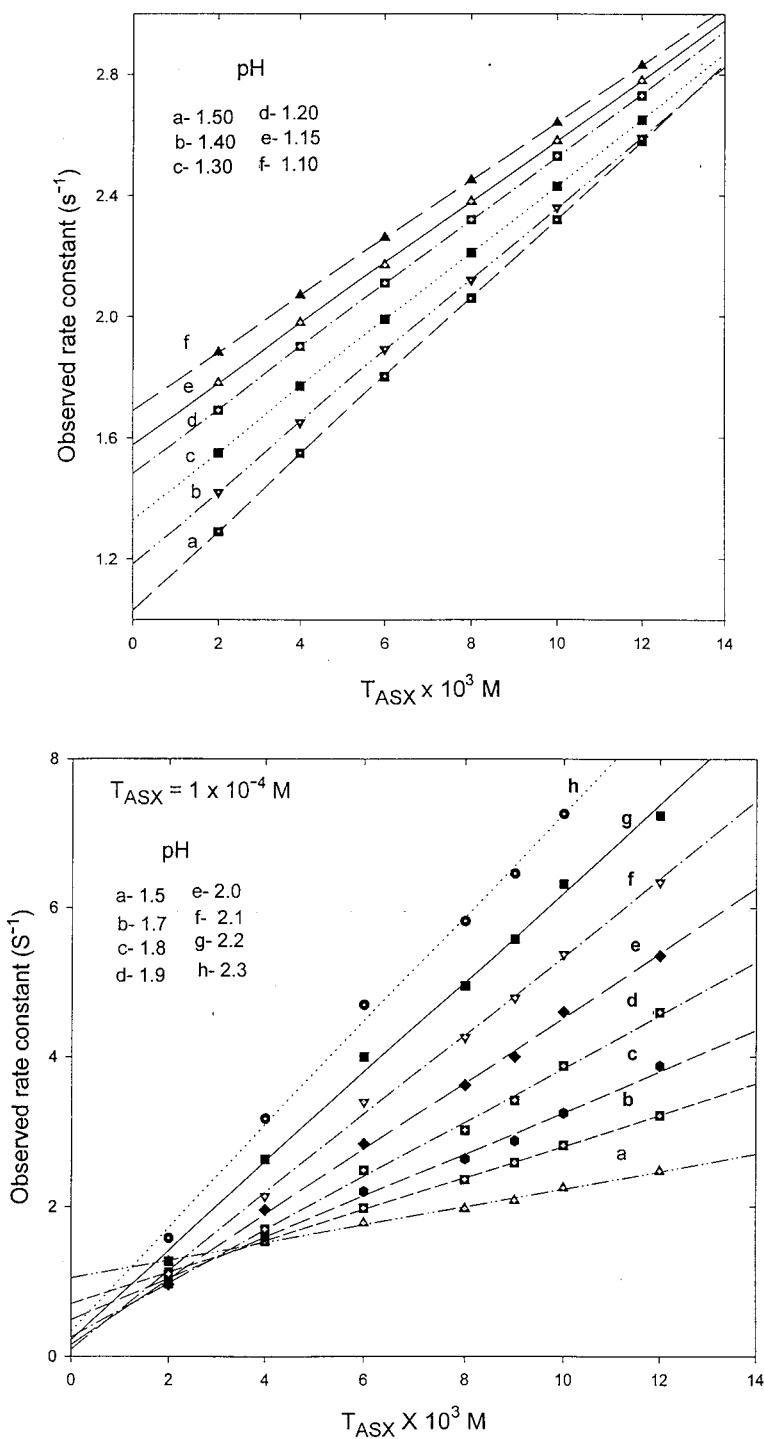


FIGURE 4 (a) The variation of the observed rate constants ( $k_{obs}$ ) as function of  $T_{ASX}$  at interpolated pH values < 1.5; (b) The variation of the observed rate constants ( $k_{obs}$ ) as function of  $T_{ASX}$  at interpolated pH values > 1.5.

TABLE II The values of A and B as a function of  $[H^+]$  for Fe(III)-ASX system

$pH^a$	$[H^+] \times 10^2 M$	$A_i$ ( $s^{-1}$ )	$[H^+]^{-1}$ ( $M^{-1}$ )	$B_i \times 10^{-3}$ ( $s^{-1}M^{-1}$ )	$BQ_3 \times 10^{-3}$	$Q_2$	$A_i \times Q_2$	$(BQ_3((H) + K_{1h}) / (H)^{-1}) 10^{-2}$
1.10	7.94	1.70	12.6	0.94	0.95	3.63	6.170	9.56
1.15	7.08	1.58	14.1	1.00	1.01	3.34	5.280	10.17
1.20	6.31	1.50	15.8	1.03	1.04	3.09	4.640	10.48
1.30	5.01	1.33	20.0	1.10	1.12	2.65	3.520	11.31
1.40	3.98	1.19	25.1	1.16	1.19	2.32	2.760	12.04
1.50	3.16	1.03	31.6	1.29	1.33	2.05	2.110	13.50
1.60	2.51	0.84	39.8	1.64	1.70	1.83	1.540	17.32
1.70	2.00	0.70	50.1	2.10	2.19	1.66	1.160	22.42
1.80	1.58	0.50	63.1	2.75	2.90	1.52	0.760	29.88
1.90	1.26	0.25	79.4	3.63	3.92	1.42	0.360	40.69
2.00	1.00	0.10	100.0	4.46	4.86	1.33	0.133	50.92
2.10	0.79	0.09	125.9	5.30	5.89	1.26	0.113	62.46
2.20	0.63	0.08	158.5	6.22	7.10	1.21	0.097	76.39
2.30	0.50	0.07	200.0	7.26	8.55	1.17	0.082	93.68

<sup>a</sup>Interpolated values of pH from Fig. 4(a,b).

constant of (FeASX)  $\{=(FeHASX)/(FeASX)(H^+)\}$ ,  $Q_3=(1+K_{1OH}/(H^+))$  (where  $K_{1OH}=(FeOH)(H^+)/(Fe^{3+})$  is the hydrolysis constant of  $Fe^{3+}$ ),  $Q_4=k_1\alpha_0+k_2K_{1OH}\alpha_0/(H^+)+k_3\alpha_1+k_4K_{1OH}\alpha_1/(H^+)+k_5\alpha_1+k_6K_{1OH}\alpha_1/(H^+)$  (where  $\alpha_0=(H^+)^3/Q_1$  and  $\alpha_1=K_{1h}(H^+)^2/Q_1$  and  $\alpha_0/\alpha_1=(H^+)/K_{1h}$ ) and  $Q_5=k_{-1}K_{HC}(H^+)^3+k_{-2}K_{HC}(H^+)^2+k_{-3}K_{HC}(H^+)^2+k_{-4}K_{HC}+k_{-5}(H^+)^2+k_{-6}(H^+)$

The integrated form of Eq. (2) is:

$$\ln ((FeASX)_\infty / ((FeASX)_\infty - (FeASX)_t)) = kt \quad (3)$$

where  $(FeASX)_\infty$  and  $(FeASX)_t$  are the concentration of the complex species at infinite time and time  $t$  (both are directly proportional to the absorbance at a given wavelength) and  $k$  is expressed as follows:

$$k = (Q_5/Q_2) + T_{ASX}(Q_4/Q_3) \quad (4)$$

Equation (1) can be correlated with Eq. (4) such that:

$$A = Q_5/Q_2 \quad (5)$$

and

$$B = Q_4/Q_3 \quad (6)$$

Rearrangement of Eq. (5) such that,  $AQ_2=Q_5$  and plotting  $A_iQ_2$  versus  $(H)_i$  yielded a linear relationship with a significant slope (=83), which corresponds to  $k_{-6}$ , and a negative intercept. This situation indicates that at pH values  $\geq 2.0$  the backward rate reactions are practically nonexistent; these rates are much less dependent on pH. The aforementioned explanation, however, ignored the experimental errors encountered in evaluating the intercept values since they accumulated all the errors of the experimental data of the observed rate constants at various hydrogen ion concentrations. In addition, there is a possibility that the reaction mechanism described in Scheme 1, could include the formation of  $Fe(ASX)_2(H)_2$  shown in the distribution

diagram of Fe(III) complex species at pH values greater than 1.5, Fig. 3a, although, the observed rate constants are not quadratically dependent on  $T_{ASX}$ . Another possibility is the formation of intermediate mixed ligand complex species such as Fe(OH)(ASXH<sub>2</sub>) which was not accounted for in Scheme 1. On the other hand, upon the rearrangement of Eq. (6) the following equation is obtained:

$$BQ_3((H) + K_{1h})/(H) = k_1 + (k_2K_{1OH} + k_3K_{1h} + k_5K_{1h})(H)^{-1} + (k_4K_{1OH}K_{1h} + k_6K_{1OH}K_{1h})(H)^{-2} \quad (7)$$

If the left side of Eq. (7) is plotted against  $(H)^{-1}$  a straight line is obtained with a slope equal to  $(47 \pm 1)$  and an intercept equal to  $(2 \pm 1) \times 10^2$ . This conclusion indicates that reactions a, b, c, and e are significant in the formation of the final product of Fe(III)-ASX system. The rate constants of these reactions can be calculated i.e.,  $k_1 = 2 \times 10^2 \text{ l}(\text{mol.s})^{-1}$ , and  $k_2$ ,  $k_3$ , and  $k_5$  may be predicted if one assumes that one of the terms  $k_2K_{1OH}$ ,  $k_3K_{1h}$ , or  $k_5K_{1h}$  is much greater than the other two terms such that  $k_2 = 5 \times 10^4 \text{ l}(\text{mol.s})^{-1}$ ,  $k_3 = k_5 = 9.5 \times 10^4 \text{ l}(\text{mol.s})^{-1}$ . It may be concluded that these four reactions are the main reaction steps leading to the formation of the final product of ASX-Fe(III) system.

### Kinetics of the Fe(III)-GLX System

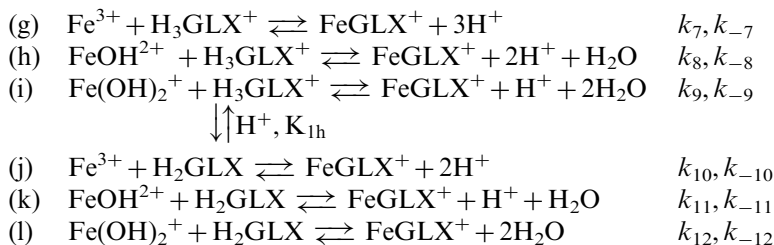
One rate step was also observed in the kinetic study of Fe(III) reaction with GLX in the pH range  $\sim 1.3$ – $2.4$ . Figure 5(a) shows the variation of  $k_{\text{obs}}$  as function of pH at various  $T_{\text{GLX}}$  while Fig. 5(b) shows  $k_{\text{obs}}$  as function of  $T_{\text{GLX}}$  at interpolated values of pH. The data obtained can be expressed as follows:

$$k_{\text{obs},i} = A'_i + B'_i T_{\text{GLX}} \quad (8)$$

Where  $A'$  and  $B'$  are the intercepts and slopes of the linear curves shown in Fig. 5(b).  $A'$  is almost a constant value ( $\sim 0.5$ ), whereas  $B'$  values are pH dependent; their values are listed in Table III. The predominant species in the solution of glutamate- $\gamma$ -hydroxamate are  $\text{H}_3\text{GLX}^+$  and  $\text{H}_2\text{GLX}$ , while Fe(III) is aquated  $\text{Fe}^{3+}$ ,  $\text{Fe}(\text{OH})^{2+}$ , and  $\text{Fe}(\text{OH})_2^+$  species.

Scheme 2 illustrates the mechanism of reaction between Fe(III) and GLX:

#### Scheme 2



The rate equation describing the mechanism in Scheme 2 can be expressed similarly to Fe(III)-ASX system as follows where some of the charges are omitted for simplicity:

$$d(\text{FeGLX})/dt = T_{\text{Fe}} - (\text{FeGLX})/Q_6 - (\text{FeGLX})((T_{\text{GLX}}Q_7)/Q_6 + Q_8) \quad (9)$$

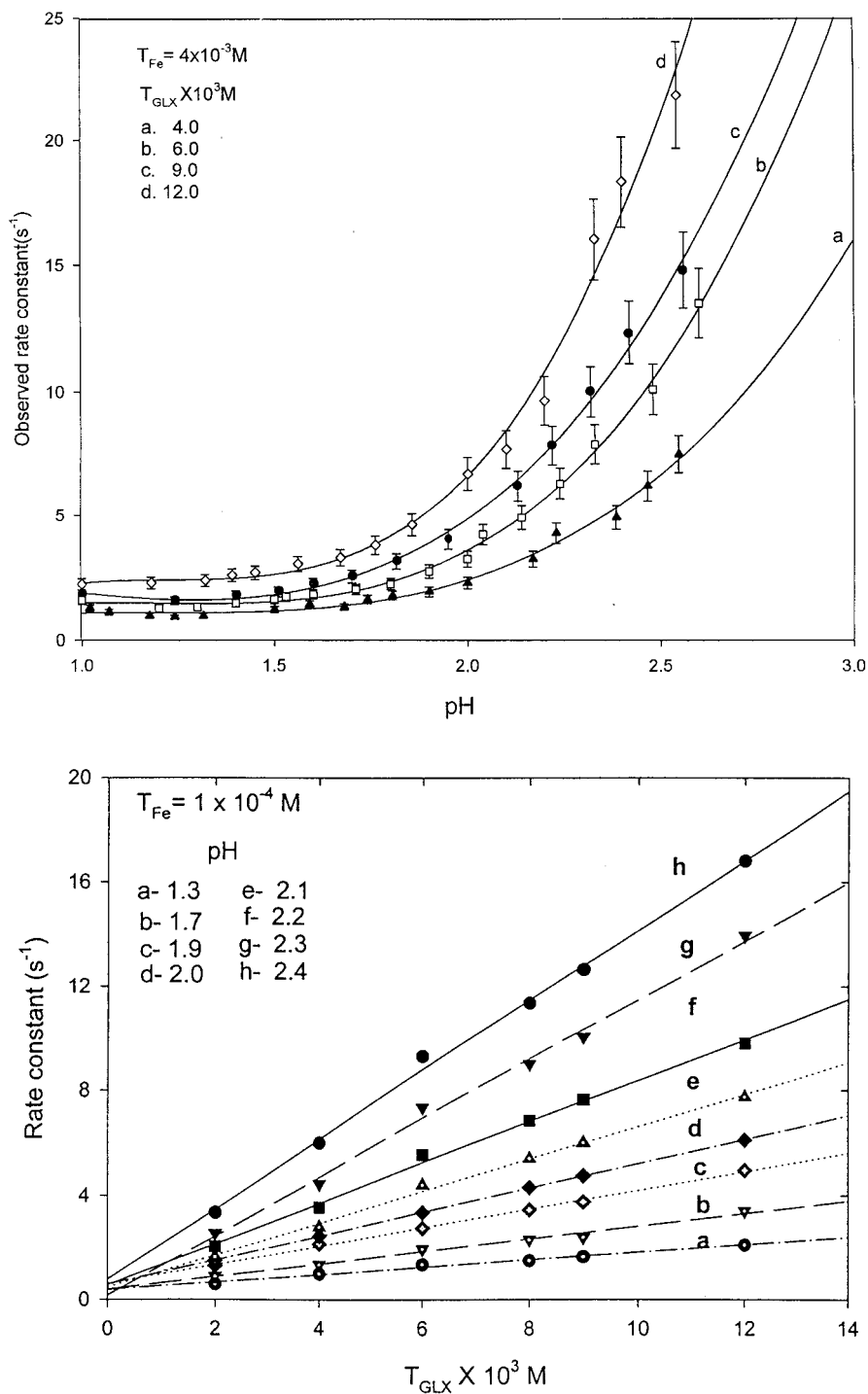


FIGURE 5 (a) The variation of  $k_{obs}$  as function of pH at a fixed wavelength ( $= 450 \text{ nm}$ ), constant  $I$  ( $0.15 \text{ M NaCl}$ ) and constant  $T$  ( $= 25^\circ \text{C}$ ) at different  $T_{GLX}$  for Fe(III)-GLX system; (b) The variation of the observed rate constants ( $k_{obs}$ ) as function of  $T_{GLX}$  at interpolated pH values.

TABLE III The values of  $B'$  as a function of  $[H^+]$  for Fe(III)-GLX

pH	$H \times 10^2$	$(H)^{-1}$	$B' \times 10^{-2}$	$Q_6$	$B'Q_6 \times 10^{-2}$	$\alpha_0$	$(B'Q_6/\alpha_0)10^{-2}$
1.3	5.00	20.00	1.5	1.02	1.53	0.903	1.694
1.4	3.98	25.12	1.6	1.02	1.63	0.881	1.850
1.5	3.16	31.65	1.8	1.03	1.85	0.855	2.164
1.6	2.51	39.84	2.0	1.04	2.08	0.824	2.524
1.7	2.00	50.00	2.3	1.045	2.41	0.788	3.058
1.8	1.58	63.29	3.0	1.057	3.17	0.746	4.249
1.9	1.26	79.37	3.7	1.071	3.96	0.701	5.649
2.0	1.00	100.00	4.7	1.090	5.12	0.651	7.865
2.1	0.79	126.58	6.15	1.114	6.85	0.595	11.513
2.2	0.63	158.73	8.00	1.143	9.14	0.540	16.926
2.3	0.50	200.00	10.6	1.180	12.50	0.482	25.934
2.4	0.40	250.00	12.2	1.225	14.94	0.427	34.988

\*Interpolated values of pH obtained from Figs. 5(a and b).

where

$$T_{GLX} = \sum_{i=0-3} [GLXH_i],$$

$$T_{Fe} = \sum_{i=0,1, j=0,1, k=0,1} [Fe(OH)_i(GLX)_j(H)_k],$$

$$Q_6 = (1 + K_{1OH}/(H) + K_{1OH}K_{2OH}/(H)^2)$$

$$Q_7 = \alpha_0\{k_7 + (k_8K_{1OH} + k_{10}K_{1h})(H^+)^{-1} + (k_9K_{1OH}K_{2OH} + k_{11}K_{1h}K_{1OH})(H^+)^{-2} + k_{12}K_{1h}K_{1OH}K_{2OH}(H^+)^{-3}\}$$

$$Q_8 = \{k_{-7}(H^+)^3 + k_{-8}(H^+)^2 + k_{-9}(H^+) + k_{-10}(H^+)^2 + k_{-11}(H^+) + k_{-12}\}$$

The integration of Eq. (9) has the general form of Eq. (3) obtained for Fe(III)-ASX system where  $k_{obs}$ , in this case, can be expressed as follows:

$$k_{obs} = Q_8 + T_{GLX}Q_7/Q_6 \quad (\text{at } pH_i) \tag{10}$$

If Eq. (10) is correlated with Eq. (8); the following are obtained:

$$A' = Q_8, \tag{11}$$

and

$$B' = Q_7/Q_6 \tag{12}$$

$A'$  was found to be more or less constant within experimental errors at various pH values and is equal to ( $\sim 0.5$ ) which indicates that the only backward rate constant of appreciable magnitude is  $k_{-12}$ . On the other hand, if  $B'$  is multiplied by  $Q_6$  such that

$$B'Q_6 = Q_7 \tag{13}$$

TABLE IV Summary of the rate constants and their magnitudes obtained in this work and other pertinent systems

<i>System Species</i>	<i>Fe Species</i>	<i>Rate Constants</i>	<i>Magnitude(l/mol.s)</i>	<i>Reference</i>
Fe-ASX-H	Fe <sup>3+</sup>	$k_1, k_{-1}$	$\sim 2 \times 10^2, \sim 0$	This work
		$k_3, k_{-3}$	$\sim 1 \times 10^5, \sim 0$	
Fe-ASX	FeOH <sup>2+</sup>	$k_2, k_{-2}$	$\sim 5 \times 10^4, \sim 0$	This work
	Fe <sup>3+</sup>	$k_5, k_{-5}$	$\sim 1 \times 10^5, \sim 0$	
Fe-GLX	FeOH <sup>2+</sup>	$k_6, k_{-6}$	$-, \sim 83$	This work
	Fe <sup>3+</sup>	$k_{10}, k_{-10}$	$8 \times 10^2, \sim 0$	
	FeOH <sup>2+</sup>	$k_8$ or $k_{11}$	$4 \times 10^3$ or $1 \times 10^4$	
		$k_{-8}$ or $k_{-11}$	$\sim 0$ , or $\sim 0$	
Fe-GX-H GX = glycinehydroxamate	Fe(OH) <sub>2</sub> <sup>+</sup>	$k_9$ or $k_{12}$	$9 \times 10^4$ or $\sim 0$	[12]
		$k_{-9}$ or $k_{-12}$	$\sim 0, 0.5$	
	Fe <sup>3+</sup>	$k_1, k_{-1}$	$2 \times 10^2, \sim 105$	
Fe-GX	FeOH <sup>2+</sup>	$k_2, k_{-2}$	$3 \times 10^4, \sim 1$	[12]
	Fe(OH) <sub>2</sub> <sup>+</sup>	$k_3, k_{-3}$	$1 \times 10^4, \sim 3 \times 10^{10}$	
	Fe <sup>3+</sup>	$k_4, k_{-4}$	$1 \times 10^3, 6 \times 10^4$	
	FeOH <sup>2+</sup>	$k_5, k_{-5}$	$3 \times 10^4, 2 \times 10^3$	
	Fe(OH) <sub>2</sub> <sup>+</sup>	$k_6, k_{-6}$	$1 \times 10^4, \sim 3$	

and if  $B'Q_6/\alpha_0$  is plotted against  $(H^+)^{-1}$  a quadratic equation is obtained where the coefficients were found to have the following values:

$$k_7 = 44 \pm 48$$

$$(k_8 K_{1OH} + k_{10} K_{1h}) = 4 \pm 1$$

$$(k_9 K_{1OH} K_{2OH} + k_{11} K_{1h} K_{1OH}) = (4 \pm 0.4) \times 10^{-2}$$

The values of  $k_8, k_9, k_{10}$ , and  $k_{11}$  can be estimated if one term is ignored with respect to the other in the coefficients of the quadratic equation i.e.,  $k_8 K_{1OH} \gg k_{10} K_{1h}$  and  $k_9 K_{1OH} K_{2OH} \gg k_{11} K_{1h} K_{1OH}$  and vice versa such that  $k_8, k_9, k_{10}$ , and  $k_{11}$  are equal to  $4 \times 10^3, 9 \times 10^4, 8 \times 10^2$ , and  $1 \times 10^4$  (l(mol.s)<sup>-1</sup>), respectively. This conclusion has shown that reactions (h), (i), (j) and (k) contribute significantly to the complex formation in the Fe(III)-GLX system.

Table IV summarizes the values of the rate constants obtained in this work with other pertinent system constants. It seems that Fe(III)-ASX system is kinetically more reactive than that of Fe(III)-GLX as evidenced by the higher magnitudes of their rate constants.

## CONCLUSIONS

The values of the rate constants obtained in this work are in the range of the values of the usual substitution reactions for water exchange by the ligand in the octahedrally solvated Fe(III) species (i.e.  $10^2 - 10^4$ ) [11]. The labilizing effect of coordinated (OH)<sup>-</sup> in the species  $\{Fe(H_2O)_5(OH)\}^{+2}$  and  $\{Fe(H_2O)_4(OH)_2\}^{+}$  over the hexaaqua ions,  $Fe(H_2O)_6^{3+}$ , enhance substitution of the water by the ligand. Although the reactivity of the  $\{Fe(H_2O)_5(OH)\}^{+2}$  species is well documented, that of  $\{Fe(H_2O)_4(OH)_2\}^{+}$  is not. The reaction mechanism for the system Fe(III)-GLX clearly shows the dependence on the presence of  $\{Fe(H_2O)_5(OH)\}^{+2}$  as well as on  $\{Fe(H_2O)_4(OH)_2\}^{+}$ . The presence of an electron-donating group in the inner coordination shell usually labilizes

coordinated water to perform water exchange with the ligand [6]. The subsequent loss of  $\text{OH}^-$  is further enhanced by the protonated ligands. One should expect that subsequent ring closure steps are more rapid (kinetically cannot be detected by stopped flow techniques) due to the labilizing effect of the hydroxamate in the inner shell in much the same way that  $\text{OH}^-$  enhances coordinated water lability in  $\{\text{Fe}(\text{H}_2\text{O})_5(\text{OH})\}^{+2}$  and  $\{\text{Fe}(\text{H}_2\text{O})_4(\text{OH})_2\}^+$ . Of course, these steps depend on the denticity of the ligand and its architecture. Further ligand coordination (Table I) and subsequent ring closures are rapid relative to the initial chelate ring formation and often not kinetically detectable by stopped-flow techniques.

The rate constants for the formation of the first complex in the Fe(III)-ASX system are  $\sim 10$  to  $\sim 100$  times more than for Fe(III)-GLX which may imply that tridentate coordination of the ligands is more effective in the GLX system than in the ASX system where bidentate character is more favorable (less crowding). The result may be correlated with Fe(III)-GX system [12] where there is only bidentate chelation.

The labilizing effect of the  $\text{Cl}^-$  in the chloro complexes of Fe(III) was ignored due to its very low stability.

Although the coordinating requirements of Fe(III) are best satisfied by siderophores containing six ligating sites, e.g. desferrioxamine, giving octahedral coordination ASX and GLX do not satisfy this requirement. They both have six coordinating sites available for binding with metal ions. Due to the hard character of Fe(III), three or four sites are available for ligation, mainly the oxygen atoms of the hydroxamate and the carboxylic groups. These ligands may act as tridentate ligands at pH values less than  $\sim 4$ . If one assumes that the equilibrium species obtained in this work, Table I, could exist at higher pH values ( $> 4$ ) complexes of these stoichiometries 3:1:–2 (ASX or GLX: Fe(III): –H), Figs. 2(a,b), predominate where the ligands are bidentate. The calculated  $\text{pFe}^{3+}$  ( $-\log [\text{Fe}^{3+}]$ ) at pH of 7.4 is  $\sim 45$  (if  $T_{\text{Fe}} = 10^{-6} \text{ M}$  and  $T_{\text{L}} = 10^{-5} \text{ M}$ ) indicating the low dissociation of these complexes in a biological environment.

ASX and GLX have the advantage over siderophores of higher molecular mass in being efficiently absorbed when dosed orally by virtue of their lower molecular mass where selective accumulation of the ligand in target tissues is required. Exposure of non-target sites however, can give rise to unwanted toxicity. A serious potential problem associated with the amino hydroxamate siderophores is that, unlike the bidentate ligands, there is a chance of forming polymeric species which does not favor complex transport through cell membranes. This was proved not to be the case in the GLX and ASX-Fe(III) complexes in the pH range used, Table I. However, this does not mean that the complexes are not able to interact with other metal ions such as Cu(II) ions in the biological environment where the amino group is ready for ligation.

Although GLX and ASX are hydrophilic at the biological pH of 7.4 ( $\log P_{\text{CALC}}$  are  $-1.9$  and  $-2.4$ ; respectively, where  $P_{\text{CALC}}$  is the calculated partition coefficient obtained from the hydrophilic–lipophilic fragment constants) one should expect that lipophilicity will increase by complex formation with Fe(III) as a result of the suppression of the overall charges on the ligand. This conclusion cannot be warranted for negatively charged complex species.

It is well known that low kinetic lability is essential for limiting possible metal redistribution *in vivo* if these metal complexes are to be used in clinical treatment. The dissociation of a monomeric metal complex is generally dependent on  $[\text{L}]$ ,  $[\text{L}]^2$ ,  $[\text{L}]^3$ , and  $[\text{L}]^6$  (where  $[\text{L}]$  is the free ligand concentration) for hexadentate, tridentate, bidentate, and monodentate ligands; respectively. Hence, the dilution sensitivity to chelate



dissociation follows the order hexadentate < tridentate < bidentate < monodentate. The estimated values for the backward rate constants obtained in this work for the interaction of GLX or ASX with Fe(III) vary according to the reaction products. Table IV, shows that most of them are of small values and are much less than the other bidentate hydroxamate ligands e.g. glycinehydroxamate confirming the conclusion that GLX and ASX are mostly acting as tridentate ligands and the rate of dissociation is minimized.

### Acknowledgement

The authors would like to thank Kuwait University for the provision of grant No. SC 094 and general facility (SAF) grant No. SLC 063.

### References

- [1] G. Winkelmann, D. van der Helm and J.B. Neilands (1987). *Iron Transport in Microbes, Plants and Animals*. VCH Verlagsgesellschaft mbH, D-6940, Weinheim, Germany.
- [2] C. Hershko, A.M. Konijn and P. Aisen (Eds.) (1994). *Advances in Experimental Medicine and Biology; Progress in Iron Research*, Vol. 356, Plenum Press, New York.
- [3] A. Sigel and H. Sigel (Eds.) (1998). *Iron transport and Storage in Microorganisms, Plants, and Animals; Metal Ions in Biological Systems*, Vol. 35, Marcel Dekker, New York.
- [4] D.H. Howard (1999). Acquisition, Transport, and Storage of Iron by Pathogenic Fungi. *Clin. Microbial. Rev.*, **12**(3), 394–404.
- [5] M.S. El-Ezaby, H.M. Marafie, M.M. Hassan and H.M. Abu Soud (1986). *Inorg. Chim. Acta*, **123**, 53.
- [6] M.S. El-Ezaby and M.M. Hassan (1988). *J. Inorg. Biochem.*, **34**, 241.
- [7] N.M. Shuaib and M.S. El-Ezaby (1995). *Polyhedron*, **14**(13–14), 1965.
- [8] J.L. Beltran, R. Codony and M.D. Prat (1993). *Anal. Chim. Acta*, **276**, 441.
- [9] E. Farkas, D.A. Brown, R. Cittaro and W.K. Olass (1993). *J. Chem. Soc. Dalton Trans.*, 2803.
- [10] N.M. Shuaib, H.M. Marafie, M.M. Hassan and M.S. El-Ezaby (1987). *J. Inorg. Biochem.*, **31**, 171.
- [11] R.G. Wilkins (1991). *Kinetics and Mechanism of Reactions of Transition Metal Complexes*, 2nd Edn. VCH Verlagsgesellschaft mbH, Germany.
- [12] M.S. El-Ezaby and M.M. Hassan (1985). *Polyhedron*, **4**(3), 429.

### APPENDIX

The derivation of Eq. (2) can be done as follows:

$$\begin{aligned}
 d((FeASX) + (FeHASX))/dt &= k_1(Fe^{3+}) + k_2(Fe(OH))(ASXH_3) + (k_3(Fe^{3+}) \\
 &+ k_4(Fe(OH) + k_5(Fe^{3+}) + k_6(Fe(OH)^{+2}))(ASXH_2) - (FeHASX)\{k_{-1}(H^+)^2 \\
 &+ k_{-2}(H^+) + k_{-3}(H^+)\} - (FeASX)\{k_{-4} + k_{-5}(H^+)^2 + k_{-6}(H^+)\}
 \end{aligned} \quad (A1)$$

Equation (A1) can be modified to Equation (2) if the following equations are taken in consideration:

$$\begin{aligned}
 T_{ASX} &\approx \sum_{i=0-3} [ASXH_i] \quad (\text{since } T_{ASX} \gg T_{Fe}) \\
 T_{Fe} &= \sum_{i=0,1, j=0,1, k=0,1} [Fe(OH)_i(ASX)_j(H)_k] \approx (Fe^{3+}) + K_{1OH}(Fe^{3+})/(H^+) \\
 &+ (FeASX) + (FeHASX) \quad (\text{where } K_{1OH} = (Fe(OH)^{+2})(H^+)/(Fe^{3+})) \\
 \alpha_0 &= (H^+)^3/Q_1 \text{ and } \alpha_1 = K_{1h}(H^+)^2/Q_1 \text{ and } \alpha_0/\alpha_1 = (H^+)/K_{1h}
 \end{aligned}$$

where  $Q_1 = (H^+)^3 + K_{1h}(H^+)^2 + K_{1h}K_{2h}(H^+) + K_{1h}K_{2h}K_{3h} \approx (H^+)^3 + K_{1h}(H^+)^2$  (in the pH range used) and  $K_{1h}$ ,  $K_{2h}$ ,  $K_{3h}$  are the deprotonation constants of  $(ASXH_3)^+$ .

$$Q_2 \frac{d((FeASX)/dt)}{dt} = T_{ASX}Q_4((T_{Fe} - Q_2(FeASX)/Q_3 - (FeASX)Q_5) \quad (A2)$$

or (at a given pH)

$$\frac{d((FeASX)/dt)}{dt} = T_{ASX}Q_4T_{Fe}/Q_2Q_3 - (FeASX)(T_{ASX}Q_2Q_4/Q_3 + Q_5)/Q_2$$

where

$$\begin{aligned} Q_2 &= (1 + K_{HC}(H^+)) \quad (\text{where } K_{HC} \text{ is the protonation constant of } (FeASX) \\ &\quad \{ = (FeHASX)/(FeASX)(H^+) \}, \\ Q_3 &= (1 + K_{1OH}/(H^+)), \quad \text{and} \\ Q_4 &= k_1\alpha_0 + k_2K_{1OH}\alpha_0/(H^+) + k_3\alpha_1 + k_4K_{1OH}\alpha_1/(H^+) + k_5\alpha_1 + k_6K_{1OH}\alpha_1/(H^+) \end{aligned}$$

(where  $\alpha_0 = (H^+)^3/Q_1$  and  $\alpha_1 = K_{1h}(H^+)^2/Q_1$  and  $\alpha_0/\alpha_1 = (H^+)/K_{1h}$ ).

At infinite time

$$\begin{aligned} \frac{d((FeASX)/dt)}{dt} &= 0, \quad \text{and} \\ T_{ASX}Q_4T_{Fe}/Q_2Q_3 &= (FeASX)_\infty (T_{ASX}Q_2Q_4/Q_3 + Q_5)/Q_2 \end{aligned} \quad (A3)$$

where  $(FeASX)_\infty$  is the concentration of the complex species at infinite time and

$$Q_5 = k_{-1}K_{HC}(H^+)^3 + k_{-2}K_{HC}(H^+)^2 + k_{-3}K_{HC}(H^+)^2 + k_{-4}K_{HC} + k_{-5}(H^+)^2 + k_{-6}(H^+)$$

On substituting Eq. (A3) in Eq. (A2) one can obtain the following equation:

$$\begin{aligned} \frac{d((FeASX)/dt)}{dt} &= (FeASX)_\infty((T_{ASX}Q_4Q_2/Q_3 + Q_5)/Q_2) \\ &\quad - (FeASX)_t((T_{ASX}Q_4Q_2/Q_3 + Q_5)/Q_2) \end{aligned} \quad (A4)$$

where  $(FeASX)_t$  is the concentration of the complex species at time  $t$ .

The integrated form of Eq. (A4) is as follows:

$$\ln ((FeASX)_\infty / ((FeASX)_\infty - (FeASX)_t)) = kt \quad (A5)$$

where  $(FeASX)_t$  and  $(FeASX)_\infty$  are directly proportional to the absorbance at time  $t$  and infinite time  $t_\infty$ , respectively, and  $k = (Q_5/Q_2) + T_{ASX}(Q_4/Q_3)$  which is comparable to the observed rate constants.

The same treatment can be followed for the other Fe(III)-GLX system.